

# A Feature Fusion Approach to Classify Diabetic Retinopathy with Modified Support Vector Machine

Karthikeyan R.\* and Alli P.

CSE, PSNA College of Engineering and Technology, Dindigul, Tamilnadu, INDIA  
Department of CSE, Velammal College of Engineering and Technology, Madurai, Tamilnadu, INDIA  
\*alli\_rajus@yahoo.com

## Abstract

Diabetic Retinopathy (DR) is the continuous pathologic alteration in the microvasculature of retina that can lead to regions of retinal non-perfusion, increase in vascular permeability, as well as pathological proliferation of vessels of retina. Therefore, it is helpful to acquire reliable assessment for diabetes patients. Currently, various phases of DR are detected by retinal inspection applying indirect bio-microscopy by senior ophthalmology specialists. In this paper, morphological image processing and Support Vector Machine (SVM) methods were applied for the automatic analysis of eye well-being. The feature subset selection, accompanied with the parameter selection in the SVM learning process considerably improves the classification accuracy. In this work, the SVMs are optimized with Glowworm Swarm Optimization (GSO) for optimal feature and parameter selection. In this work, three classes are recognized: normal retina, mild Non-Proliferative Diabetic Retinopathy (NPDR), and Proliferative Diabetic Retinopathy (PDR). Features including blood vessels, color and exudates were extracted using Wavelets, Color histogram and Fuzzy C Means Segmentation respectively. Five groups were diagnosed: normal retina, mild Non-Proliferative Diabetic Retinopathy (NPDR), moderate NPDR, severe NPDR, and Proliferative Diabetic Retinopathy (PDR). Four notable features blood vessels, microaneurysms, exudates, as well as haemorrhages were obtained from raw images with the help of image processing methods, then SVM was used for classification. Investigational outcomes reveal that the proposed technique accomplished improved classification.

**Keywords:** Diabetic Retinopathy (DR), Proliferative Diabetic Retinopathy (PDR), Feature Extraction, Feature Selection, Support Vector Machine (SVM) and Glowworm Swarm Optimization (GSO).

## Introduction

Diabetes mellitus is a disorder of carbohydrate metabolism caused because of impaired production or absolute absence of the hormone insulin, leading to increased blood sugar levels. Due to increased blood sugar level (hyperglycemia) all vital organs are affected including brain, eyes, and

kidney. Diabetic Retinopathy (DR) affects the retinal vascular system, leading to impairment of the retina and ultimately loss of sight.

DR can occur even as early as 20 years or as late as 74 years. The defect is increasing proportionately and is becoming a glitch to the wellbeing of the community. In UK, 3 million people are assessed to be affected with diabetes and this number can probably go up in 2-3 decades.<sup>1</sup>

Diabetics patients should go through routine eye testing to screen the onset of DR or to rule out DR. Usually retinal images are taken and Figure 1 depicts instances of such images. Numerous phases of retinal images provide the stage of DR which are evaluated by physicians. This regular evaluation can help the diabetics in large but is time consuming and costly task. Automated detection system will be advantageous to the physicians in assessing the retinal images for DR.

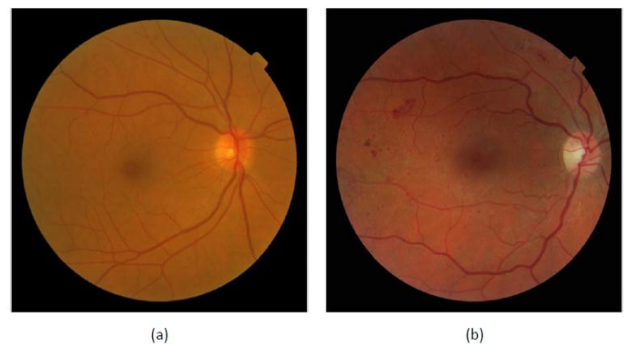


**Figure 1: (a) Healthy retinal image. (b) Retinal image with DR.**

DR can either be PDR (Proliferative Diabetic Retinopathy) or NPDR (Non-Proliferative Diabetic Retinopathy). Based on the particular DR traits, the phases of DR are categorized. The three subclasses of NPDR and PDR are as follows:

- **Mild NPDR:** Minimum one microaneurysm which has or doesn't have trace of retinal haemorrhages, hard exudates, cotton wool spots or the venous loops. About 40% population who possess diabetes show least DR symptoms.
- **Moderate NPDR:** Many microaneurysms as well as retinal haemorrhages exists. A finite quantity as well as cotton wool spots of venous beading. 16% of the patients with mild NPDR may evolve PDR in an year.
- **Severe NPDR:** is represented using one among the below (4-2-1 rule) characters: (1) plenty haemorrhages as well as microaneurysms in 4 retinal quadrants (2)

venous beading in 2 or more quadrants (3) Intra retinal microvascular abnormalities in at least 1 quadrant. Severe NPDR possess a 50% possibility to develop as PDR in an year.

1. Other than micro-aneurysms, a number of hemorrhages are present in all quadrants of the retina;
2. Presence of venous beading in two or more quadrants of the retina;
3. Presence of intra-retinal microvascular aberrations in at least one quadrant.

Again 50% of diabetics with this type of NPDR can go into PDR in less than a year.

- **PDR:** This is the extreme level; signals that are forwarded by the retina to nourish, kindle the prosperity of new blood vessels. They don't show any signs or else losing eyesight. Yet, due to thin as well as delicate walls, they are under a higher risk they might leak blood. The blood leakage could contaminate the vitreous gel and can produce complicated loss of vision or maybe blindness. Around 3% of people, who have this condition, could come across critical loss of vision<sup>3</sup>

To diagnose DR various implements such as linear ophthalmoscope, PAN ophthalmoscope, binocular lengthy ophthalmoscope, slit lamp and fundus camera are used. The primary technique is mydriatic, that is requires dilatation of the pupils. The other type is non-mydriatic whose application is stress-free, keeps the sick person pleasant and unless essential, dilation of pupil is not done. Digital pictures is obtained through the fundus camera 2which can be viewed instantly<sup>2</sup>.

The earliest or the initial change which can be evaluated by a technician in DR is micro-aneurysm, which are seen as small red dots. Other indications include hemorrhages or red abrasions that are formed because of the break in the small blood vessels inside the retina. Yellow-white abrasions which are formed by plasma leak from the capillaries called exudates. If the exudates are present in less than One Discus Distance (IDD) of fovea, then it is called 'exudative maculopathy.'

Three major components in the retina are: Neuronal, Glial and Vascular.

- Neuronal is responsible for the vision; the light is converted into electrical signals by the nerves leading to vision.
- Glial are the backing support of the retina;
- Vascular provides for the interior retina, while exterior retina is provided through dispersion of choroidal movement.

Diabetes usually causes changes in neuronal and retinal vascular components. The various factors that affect DR are age, gestation, blood pressure, hyper-viscosity, kidney problems, and anemia. It is also seen that the DR is bought about by the hyper-viscosity of the blood<sup>3</sup>.

In automated detection system, the retinal images are taken as input and using image processing techniques, the DR is detected. Algorithms are applied to process the images and features are extracted which are used to identify whether the retinal image is normal or abnormal. Machine learning algorithms are used for classification of the features. Feature selection techniques reduce the dimensionality of the extracted feature set by removing irrelevant data thus improving classification accuracy<sup>4</sup>. The optimal selection of feature subset is essential to improve accuracy and reduce computational time. In this work, a feature selection using GSO is proposed and SVM parameter optimization in DR. Section 2 reviews related work in literature. Section 3 describes methods used and Section 4 discusses experiments results. Section 5 concludes the work.

### Related Works

Hemorrhages were detected in fundus images using automated methods by Bharali et al.,<sup>5</sup>. Blood vessels in the image were identified and eliminated in the first phase and the Hemorrhage were identified in the next phase. High Resolution Fundus Image (HRF), Standard Diabetic Retinopathy Database (DIARETDB) 0, DIARETDB1, MESSIDOR were used along with local records that have both usual and pathological images.

Pires et al.,<sup>6</sup> investigated bypass lesion detection. In the proposed method, BossaNova and Fisher Vector were applied to extract features from the retinal images and directly train a classifier for DR classification. Rahim et al.,<sup>7</sup> explored the existing methods for microaneurysm detection. Various feature extraction techniques were applied on DR colour fundus images and the circular Hough transform for microaneurysm detection system, with the fuzzy histogram equalization method was used. The results conclude that the latter method significantly improved results for detecting the microaneurysms.

SVM classifiers and ANN are widely used in the detection of DR. Mane et al.,<sup>8</sup> used SVM classifier for automatic detection of red lesions in fundus images. Modified matched filtering method was used for extracting retinal vasculature and detecting candidate lesions. When tested with 89 fundus images from DIARETDB1 database, an accuracy of 96.62% was achieved. Balakrishnan et al.,<sup>9</sup> investigated DR detection using binary SVM. Texture features were extracted from the images and to improve the efficacy, a hybrid feature selection based on Particle Swarm Optimization (PSO) and Differential Evolution Feature Selection (DEFS) was proposed. Subudhi et al.,<sup>10</sup> used PSO algorithm for enhancing the images to improve the performance of filters. The blood vessels were more accurately detected with the

use of proposed method. Carnimeo & Nitti <sup>11</sup> presented a Radial Basis Probabilistic Neural Network (RBPNN) for detection of PDR in diabetic patients.

Bharali et al., <sup>12</sup> proposed an automatic computer assisted technique to detect the hemorrhages with the help of image of the fundus. Initially, blood vessels are identified and then eradicated. During the next stage, hemorrhage candidate was identified. This technique was established on High Resolution Fundus Image (HRF), Standard Diabetic Retinopathy Database (DIARETDB) 0, DIARETDB1, MESSIDOR and local databases that contain both normal as well as infected images. The presented technique proves an entire sensitivity of about 97.3%, then specificity of 98.92% in detecting hemorrhage.

Jindal <sup>13</sup> presented an adaptive optics a latest imaging method, that proved that losing the photoreceptors (specialized neurons) indicated an earlier alteration in DR. These alterations show that DR is a neurovascular syndrome. Neuroprotective agents also gave better outcomes when DR progression is delayed, particularly memantine, insulin receptor activation, as well as neurotrophic reasons. Advanced researchers in this area could assist us in finding novel therapy ideas of DR, that could either delay or terminate DR progressing in earlier stages.

Pires et al., <sup>14</sup> proposed the bypass lesion diagnosis, training a classifier in a direct manner for DR referral. Extra novelties are the usage of state of the art mid range feature for the image of retina: BossaNova as well as Fisher Vector. These features could enhance the classic bag of visualizing words and enhance the accuracy of difficult classification works. This method of direct referral was better, that achieved a region below the curve of about 96.4%, thereby decreasing the error in classification for about 40% over present state of art, provided by lesion based methods.

Rahim et al., <sup>15</sup> analysed the prevailing schemes and uses corresponding to DR screening, concentrating over the microaneurysm detecting techniques. This idea supporting scheme has an automated acquisition, screening as well as classifying the DR color fundus image, that can support in detecting as well as managing DR. Many feature extracting schemes as well as circular Hough transform were used in this microaneurysm detecting scheme, together with the fuzzy histogram equalization technique. The second technique was used in the pre-processing level of DR eye fundus images that showed enhanced outcomes to detect the micro aneurysm.

Mane et al., <sup>16</sup> explained a specific technique to detect red lesions present in fundus images automatically. This technique used latest approach to match filtering to extract the retina vasculature and to detect the candidate lesions. Characters of all of the candidate lesions are obtained and are employed in training SVM classifier. Following which

SVM grouped input image object to be in either lesion or non lesion group.

This technique was examined with the help of 89 fundus images from the DIARETDB1 database. The presented technique shows performance to be 96.42%, specificity 100% and accuracy 96.62%.<sup>2</sup>

Balakrishnan et al., <sup>17</sup> gave a hybrid techniques depended DR diagnosis. Initially preprocessing the input image with the help of green channel extraction as well as median filter occurs. Then extraction of gradient based features such as Histogram of Oriented Gradient (HOG) with Complete Local Binary Pattern (CLBP) is done. These textural features are surrounded by numerous rotations in order that edges are calculated. In order that a hybrid feature selection which blends Particle Swarm Optimization (PSO) as well as Differential Evolution Feature Selection (DEFS) is to be given to maximize the time complex. A digital SVM classifier could group the 13 normal as well as 75 abnormal images of 60 patients. At last, patients infected with DR are also categorized using Multi-Layer Perceptron (MLP). The outcomes of experiments show good accuracy in performance, sensitivity, as well as specificity compared to the prevailing techniques.

Subudhi et al., <sup>18</sup> optimized PSO protocol was made use to enhance the images with edges in order to enhance the working of filters. With the response from the thresholding to the Matched Filter (MF), the vessels were identified, however adjusting the threshold was done with the response from First-order Derivative of Gaussian (FDOG). The PSO depended improved MF response notably enhanced the performance of filters in the extraction process of structure of blood vessels. Outcomes of experiments proved that this technique which uses improved images has increased the accuracy level to about 91.1% that remains higher compared to MF as well as MF-FDOG, correspondingly. The peak signal-to-noise ratio was also found to be higher with low mean square error values in enhanced MF response. The accuracy, sensitivity, as well as specificity values are notably enhanced compared to MF, MF-FDOG, as well PSO-improved images ( $P < 0.05$ ).

Lin et al., <sup>19</sup> proposed a latest version of Cat Swarm Optimization (MCSO), which has the capability to improve search efficiency within the problem space. The basic CSO protocol was infused with a local search scheme and feature selection along with parameter optimization of SVMs. Experimental outcomes showed the superior nature of MCSO in the classification accuracy with the help of subsets having less features for provided UCI dataset, in comparison with the original CSO protocol. Also, experimental outcomes depict the fitter CSO variables as well as MCSO takes minimum time to train to get outcomes having high accuracy compared to original CSO. Hence, MCSO is suits real time uses.

Ibrahim et al.,<sup>20</sup> presented how to partition the membership functions in a fuzzy logic inference system. A clustering technique divides the membership functions by gathering similar data to form clusters, while an equalized universal techniques partition the data to predefined equal clusters.

A data adapting technique makes use of a data frequency based technique to divide every trait depending on data dissemination over that trait.

A data adapting neuro fuzzy inference schemes formulates respective rules in both fine as well as coarse distributed traits. This technique gave much beneficial rules along with much efficient classifying technique. An entire accurate level of 98.55% was observed.

Carnimeo & Nitti<sup>21</sup> proposed a PDR through a novel neural classifier depending on a Fundus Image Pre processing subsystem as well as a Radial Basis Probabilistic Neural Network (RBPNN). This technique was the initial one in its case which was pursued by diabetic patients infected. The presented classifier targets to classify a particular group of diabetic patients using their accurate preprocessed binary fundus image and also support their follow-ups and alert them in case any retinal vasculature of categorized PDR occurred

**Methodology**

In this section, the features such as areas of blood vessels, micro-aneurysms, exudates, and hemorrhages were mined off the fundus image. SVM classifier and GSO algorithm are detailed. Feature selection and parameters optimization for SVM based on GSO method is presented.

**Feature Extraction using Wavelet Co-efficient Approximation:**

The detection of blood vessels is one of the very important features in the identification of DR stages. The features are extracted using wavelet coefficients. In Discrete Wavelet Transform (DWT)<sup>22</sup>, it can approximate a

discrete signal in  $l^2(Z)^1 = \{f[n] | \sum_{n=-\infty}^{\infty} |f[n]|^2 < \infty\}$  by (1):

$$f[n] = \frac{1}{\sqrt{M}} \sum_k W_\phi[j_0, k] \phi_{j_0, k}[n] + \frac{1}{\sqrt{M}} \sum_{j=j_0}^{\infty} \sum_k W_\psi[j, k] \psi_{j, k}[n] \tag{1}$$

Here  $f[n]$ ,  $\phi_{j_0, k}[n]$  and  $\psi_{j, k}[n]$  are discrete functions defined in  $[0, M - 1]$ , totally M points. Because the sets  $\{\phi_{j_0, k}[n]\}_{k \in Z}$  and  $\{\psi_{j, k}[n]\}_{(j, k) \in Z^2, j \geq j_0}$  are orthogonal to each other. It can simply take the inner product to obtain the wavelet coefficients:

$$W_\phi[j_0, k] = \frac{1}{\sqrt{M}} \sum_n f[n] \phi_{j_0, k}[n] \tag{2}$$

$$W_\psi[j, k] = \frac{1}{\sqrt{M}} \sum_n f[n] \psi_{j, k}[n] \quad j \geq j_0$$

In equation (2) shows the approximation coefficients and detailed coefficients.

**Feature Extraction using Detection of Exudates (EX):**

The proposed technique obtained candidate EX regions by performing Fuzzy C-Means (FCM) segmentation<sup>23</sup> directly on the colour retinal images. This involved two important pre-processing steps: normalization of the images and segmentation. In hard segmentation method, crisp decisions of regions is obtained although the regions are generally not crisply defined. In fuzzy approaches, pixels can belong to multiple classes with varying degrees of membership. It segments the retinal images using a two-stage colour segmentation algorithm based on Gaussian-smoothed histogram analysis and FCMs clustering comprising a coarse and a fine segmentation step.

At the coarse stage, an initial classification is achieved through interval analysis of the zero-crossings of the histogram second derivative at multiple scales in each colour band resulting in K number of classes. In the fine stage, FCM allocates any unclassified pixels to the nearest class based on the minimization of the objective function in (3):

$$J_m(P, V) = \sum_{i=1}^c \sum_{k=1}^n (\mu_{ik})^m \|x_k - v_i\|^2 \tag{3}$$

Where P is a fuzzy partition of the data ( $x_k, k=1 \dots n$ ) and V is a vector of cluster centres ( $v_i, i=1 \dots c$ ). Also,  $\mu_{ik}$  represent the membership value of  $x_k$  to cluster i. These memberships must be between 0 and 1, and  $\mu_{ik}$  must sum to 1 for all i. The parameter m is a weight that determines the degree to which partial members of a cluster affect the clustering result. The fuzzy partitioning is carried out through an iterative optimisation in order to find both prototypes  $v_i$  and membership functions  $\mu_{ik}$  to minimise  $J_m$ . Here, m = 2 and the algorithm runs until the Euclidean distance between two successive membership values reached is 0.5.

**Feature Extraction using Color Histogram:** In a color histogram, the images are scaled to have same number of pixels, and the colors are mapped as a vector giving the number of pixels of a given color in the image<sup>15</sup>. The method used two colour channels (Red and Green) without intensity

component. A colour locus for each finding type,  $F_i$ , is defined by forming their colour histograms  $h_{F_i}(r, g)$ . The

histograms are calculated based on the intensity of the normalised pixel colours in the neighborhood (8x8).

**Support Vector Machine (SVM) Classifier:** SVM learning procedure is used for classifying images into their particular classes viz., PDR, NPDR or Normal. The SVM uses kernel for classifying data into classes. The kernels map input data into a higher dimensional feature space and a hyperplane separates the data. For instance  $(x_i, y_i)$  with  $x_i \in \mathfrak{R}^n, y_i \in [1, -1]$  for  $1 \leq i \leq n$  where n is the number of instances<sup>17</sup>, SVM's solve the following optimization problem (6):

$$\min_{w,b,\xi} \frac{1}{2} w^T w + C \sum_{i=1}^n \xi_i \tag{6}$$

Subject to (7):

$$y_i(w^T \phi(x_i)) + b \geq 1 - \xi_i, \xi_i \geq 0 \tag{7}$$

Where the decision hyperplane is a normal vector, C is the penalty parameter and  $\phi$  charts a learning example  $x_i$  to higher dimensional space. The kernel K is given by (8):

$$K(x_i, x_j) = \phi(x_i)^T \phi(x_j) \tag{8}$$

The Radial Basis Function (RBF) kernel is defined as (9):

$$K(x_i, x_j) = \exp\left(-\gamma \|x_i - x_j\|^2\right), \gamma \geq 0 \tag{9}$$

where  $\gamma$  is kernel parameter. C and  $\gamma$  to regulate the functioning of the SVM

**Glowworm Swarm Optimization (GSO) Algorithm:** With GSO, every glowworm carrying its own luciferin disperses through the defined space. The brightness of the glowworm indicates the measure of objective function, brighter the glowworm, better its position. The glowworm is restricted by its field of vision called the local decision range. The glow pursues its neighbors in the local decision range. The brighter glowworm attracts the glow. The direction of movement changes each time with choice of neighbor<sup>18</sup>. The

objective function  $J(x_i(t))$  is encoded in each glowworm i at its existing position  $x_i(t)$  with the luciferin value  $l_i$ . These values are transmitted in the neighborhood. The neighboring glowworms i comprises a comparatively greater  $l_i$  and are positioned within the dynamic decision area gets updated through formula (10) in each iteration

Local-decision range update in (10):

$$r_d^i(t+1) = \min\{r_s, \max\{0, r_d^i(t) + \beta(n_i - |N_i(t)|)\}\} \tag{10}$$

And  $r_d^i(t+1)$  is the glowworm i's local decision range in t + 1 iteration,  $n_i$  is the neighbourhood threshold, the parameter  $\beta$  affects the rate of change of the neighbourhood range.

The number of glowworm in local-decision range in (11):

$$N_i(t) = \{j : \|x_j(t) - x_i(t)\| < r_d^i; l_i(t) < l_j(t)\} \tag{11}$$

where  $x_j(t)$  and  $l_j(t)$  is the glowworm i's position and luciferin at the t iteration, the set of neighbours contains glowworms with relatively higher luciferin value and are located within a dynamic decision domain whose range  $l_i$  d r

is bounded above by a circular sensor range  $r_s$  ( $0 < r_d^i < r_s$ ). The probability  $p_{ij}(t)$  is the probability with which glowworm i selects a neighbour j and moves toward it<sup>19</sup>. Probability distribution used to select a neighbour given by (12):

$$p_{ij}(t) = \frac{l_j(t) - l_i(t)}{\sum_{k \in N_i(t)} l_k(t) - l_i(t)} \tag{12}$$

Movement update given by (13):

$$x_i(t+1) = x_i(t) + s \left( \frac{x_j(t) - x_i(t)}{\|x_j(t) - x_i(t)\|} \right) \tag{13}$$

Luciferin-update given by (14):

$$l_i(t) = (1 - \rho)l_i(t-1) + \gamma J(x_i(t)) \tag{14}$$

where  $\rho \in (0,1)$ , the parameter  $\gamma$  only scales the function fitness values,  $J(x_i(t))$  is the value of test function.

**Proposed System Architectures of Feature Selection and Parameters Optimization for SVM based on GSO:** In this section, the system architecture for selecting optimal feature subset and SVM parameter based on GSO is detailed. The figure 2 shows the steps and is discussed here.

**Step (1) Input dataset:** The dataset is split into training and testing dataset. The images of training dataset is used as input initially.

**Step (2) Data pre-processing:** All the features in the dataset is linearly scaled in the range [0, 1] by (15):

$$a' = \frac{a - \min}{\max - \min} \tag{15}$$

where a is original value, max and min are the highest and lowest value in the feature set, a' is the scaled value.

**Step (3) Choosing feature subset:** The irrelevant features are discarded to form optimal feature subset.

**Step (4) Training SVM:** The SVM is trained using the selected feature subset and varying values of  $(C, \gamma)$  and the classification accuracy is calculated.

**Step (5) Evaluating Fitness:** the fitness value is based on classification accuracy, and the number of features in the feature subset. The fitness function is evaluated using (16):

$$fit = W_A \times A + W_F \times \left( P + \left( \sum_{i=1}^{n_f} C_i \times F_i \right) \right)^{-1} \quad (16)$$

Where A - classification accuracy,  $W_A$  - weight of classification accuracy,  $F_i$  - feature value,  $W_F$  - feature weight,  $C_i$  - feature cost, P - a constant.

**Step (6) GSO phase:** Each glowworm is encoded with varying feature subset and SVM parameter values. The GSO algorithm initiates by distributing the glowworms randomly and with equal quantity of luciferin. During the iteration, the luciferin is updated, the movement is updated. These steps improve the classification accuracy of SVM.

**Step (7) Terminating Condition:** When the terminating condition is met, the process stops. In this work, the termination condition is 300 cycles.

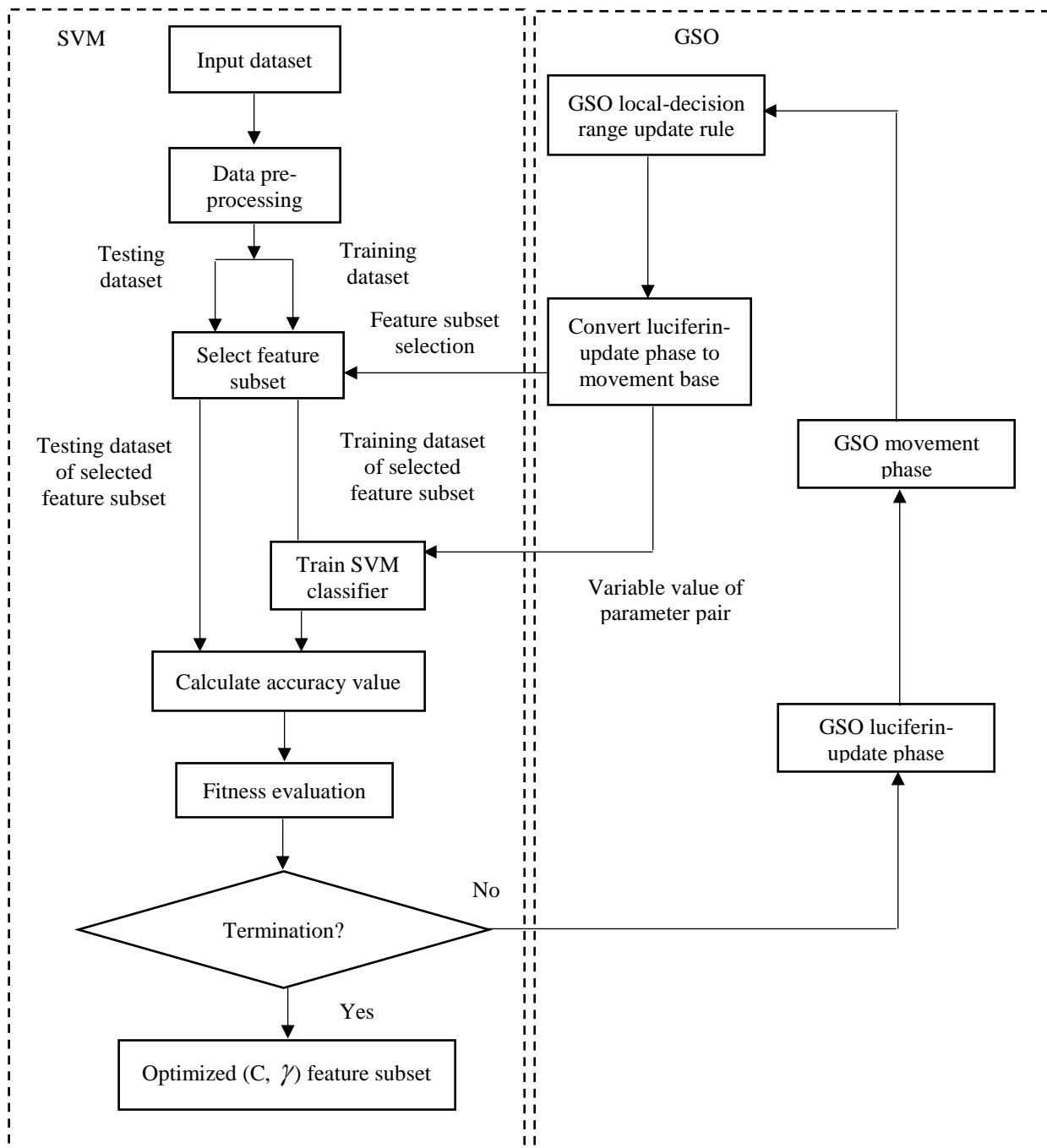


Figure 2: System architectures of feature selection and parameters optimization for SVM

**Results and Discussion**

In this section, the results of SVM with Correlation based Feature Selection (CFS) feature selection, SVM with GSO feature selection and SVM with GSO feature selection and parameter optimization methods is presented. Table 1 shows the summary of results and figure 7 to 10 shows the accuracy, sensitivity, specificity and f measure.

**Table 1**  
**Summary of Results**

	SVM with CFS feature selection	SVM with GSO feature Selection	SVM with GSO feature selection and parameter optimization
Accuracy	0.8082	0.863	0.9178
Sensitivity for Normal	0.8636	0.9091	0.9545
Sensitivity for Moderate	0.7917	0.875	0.9167
Sensitivity for Severe	0.7778	0.8148	0.8889
Specificity for Normal	0.8889	0.9149	0.9583
Specificity for Moderate	0.8696	0.913	0.9574
Specificity for Severe	0.9268	0.9535	0.9556
F Measure for Normal	0.8261	0.8696	0.9333
F Measure for Moderate	0.7755	0.8571	0.9167
F Measure for Severe	0.8235	0.8628	0.9057

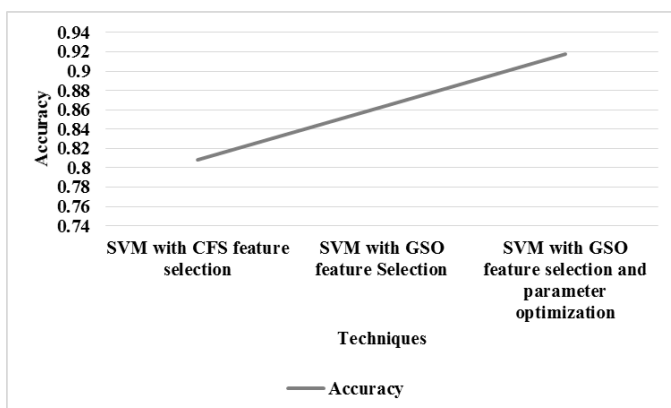


**Figure 3: Accuracy**

From the figure 3, it can be observed that the SVM with GSO feature selection and parameter optimization has higher accuracy by 12.69% for SVM with CFS feature selection and by 6.15% for SVM with GSO feature selection

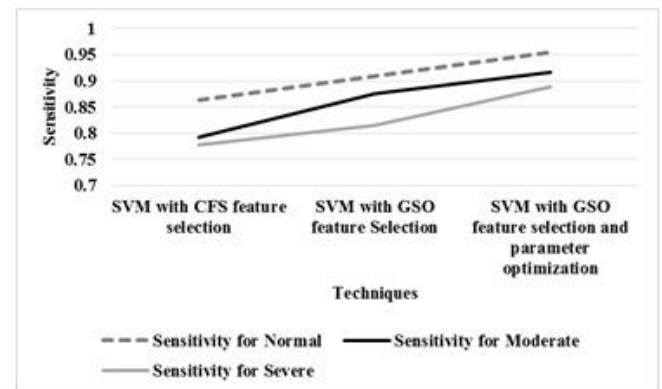


**Figure 4: Sensitivity**

From the figure 4, it can be observed that the SVM with GSO feature selection and parameter optimization has higher average sensitivity by 12.69% for SVM with CFS feature selection and by 6.01% for SVM with GSO feature selection.

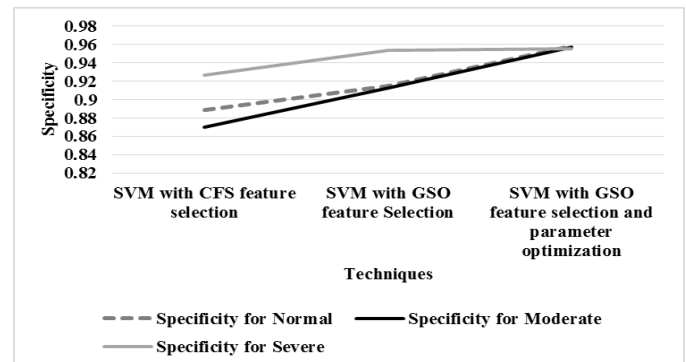


**Figure 5: Specificity**

From the figure 5, it can be observed that the SVM with GSO feature selection and parameter optimization has higher average specificity by 6.69% for SVM with CFS feature selection and by 3.18% for SVM with GSO feature selection.

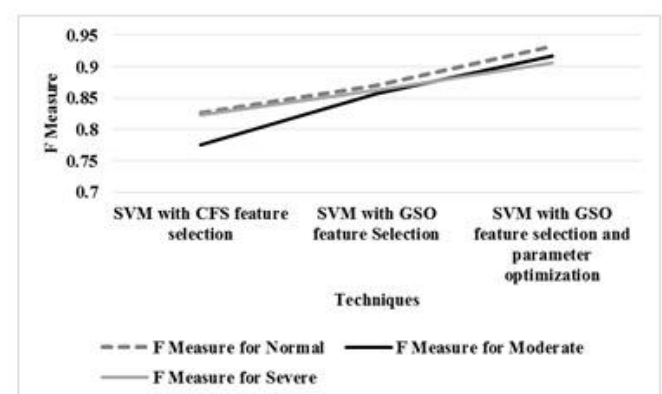


**Figure 6: F Measure**

From the figure 6, it can be observed that the SVM with GSO feature selection and parameter optimization has higher average f measure by 12.76% for SVM with CFS feature selection and by 6.21% for SVM with GSO feature selection.

## Conclusion

Digital retinal imaging is an effective technique for screening DR. Automated detection system is effective for screening large volume of images. In this work, the retinal images are classified into normal, PDR and NPDR using optimized SVMs. The GSO is applied for selecting optimal feature subset and SVM parameters. Results show that the SVM with GSO feature selection and parameter optimization has higher accuracy by 12.69% for SVM with CFS feature selection and by 6.15% for SVM with GSO feature selection

## References

1. Shaik, F., Sharma, A. K., & Ahmed, S. M. (2015). Review of Image Processing Methods on Diabetic Related Images. *International Journal of Engineering and Techniques*, **1** (4), 99-108.
2. Rahim, S. S., Palade, V., Shuttleworth, J., & Jayne, C. (2016). Automatic screening and classification of diabetic retinopathy and maculopathy using fuzzy image processing. *Brain Informatics*, **3**(4), 249-267.
3. Shaik, F., Sharma, A. K., & Ahmed, S. M. (2015). Review of Image Processing Methods on Diabetic Related Images. *International Journal of Engineering and Techniques*, **1** (4), 99-108.
4. Jagannath, M., & Adalarasu, K. (2015). Diagnosis of diabetic retinopathy from fundus image using fuzzy c-means clustering algorithm. *J Inst Integr Omics Appl Biotechnol*, **6**(4), 3-9.
5. Lupaşcu, C., Tegolo, D., & Trucco, E. (2009). A comparative study on feature selection for retinal vessel segmentation using FABC. In *Computer Analysis of Images and Patterns* (pp. 655-662). Springer Berlin/Heidelberg.
6. Bharali, P., Medhi, J. P., & Nirmala, S. R. (2015, July). Detection of hemorrhages in diabetic retinopathy analysis using color fundus images. In *Recent Trends in Information Systems (ReTIS), 2015 IEEE 2nd International Conference on* (pp. 237-242). IEEE.
7. Pires, R., Avila, S., Jelinek, H. F., Wainer, J., Valle, E., & Rocha, A. (2017). Beyond lesion-based diabetic retinopathy: a direct approach for referral. *IEEE journal of biomedical and health informatics*, **21**(1), 193-200.
8. Rahim, S. S., Jayne, C., Palade, V., & Shuttleworth, J. (2016). Automatic detection of microaneurysms in colour fundus images for diabetic retinopathy screening. *Neural Computing and Applications*, **27**(5), 1149-1164.
9. Mane, V. M., Kawadiwale, R. B., & Jadhav, D. V. (2015, June). Detection of Red lesions in diabetic retinopathy affected fundus images. In *Advance Computing Conference (IACC), 2015 IEEE International* (pp. 56-60). IEEE.
10. Balakrishnan, U., Venkatachalapathy, K., & S Marimuthu, G. (2015). A Hybrid PSO-DEFS Based Feature Selection for the Identification of Diabetic Retinopathy. *Current diabetes reviews*, **11**(3), 182-190.
11. Subudhi, A., Pattnaik, S., & Sabut, S. (2016). Blood vessel extraction of diabetic retinopathy using optimized enhanced images and matched filter. *Journal of Medical Imaging*, **3** (4), 044003-044003.
12. Carnimeo, L., & Nitti, R. (2015, August). On classifying diabetic patients' with proliferative retinopathies via a radial basis probabilistic neural network. In *International Conference on Intelligent Computing* (pp. 115-126). Springer International Publishing.
13. Bharali, P., Medhi, J. P., & Nirmala, S. R. (2015, July). Detection of hemorrhages in diabetic retinopathy analysis using color fundus images. In *Recent Trends in Information Systems (ReTIS), 2015 IEEE 2nd International Conference on* (pp. 237-242). IEEE.
14. Jindal, V. (2015). Neurodegeneration as a primary change and role of neuroprotection in diabetic retinopathy. *Molecular neurobiology*, **51**(3), 878-884.
15. Pires, R., Avila, S., Jelinek, H. F., Wainer, J., Valle, E., & Rocha, A. (2017). Beyond lesion-based diabetic retinopathy: a direct approach for referral. *IEEE journal of biomedical and health informatics*, **21**(1), 193-200.
16. Rahim, S. S., Jayne, C., Palade, V., & Shuttleworth, J. (2016). Automatic detection of microaneurysms in colour fundus images for diabetic retinopathy screening. *Neural Computing and Applications*, **27**(5), 1149-1164.
17. Mane, V. M., Kawadiwale, R. B., & Jadhav, D. V. (2015, June). Detection of Red lesions in diabetic retinopathy affected fundus images. In *Advance Computing Conference (IACC), 2015 IEEE International* (pp. 56-60). IEEE.
18. Balakrishnan, U., Venkatachalapathy, K., & S Marimuthu, G. (2015). A Hybrid PSO-DEFS Based Feature Selection for the Identification of Diabetic Retinopathy. *Current diabetes reviews*, **11**(3), 182-190.
19. Subudhi, A., Pattnaik, S., & Sabut, S. (2016). Blood vessel extraction of diabetic retinopathy using optimized enhanced images and matched filter. *Journal of Medical Imaging*, **3** (4), 044003-044003.
20. Lin, K. C., Huang, Y. H., Hung, J. C., & Lin, Y. T. (2015). Feature selection and parameter optimization of support vector machines based on modified cat swarm optimization. *International Journal of Distributed Sensor Networks*, **11**(7), 365869.
21. Ibrahim, S., Chowriappa, P., Dua, S., Acharya, U. R., Noronha, K., Bhandary, S., & Mugasa, H. (2015). Classification of diabetes maculopathy images using data-adaptive neuro-fuzzy inference classifier. *Medical & biological engineering & computing*, **53**(12), 1345-1360.
22. Carnimeo, L., & Nitti, R. (2015, August). On classifying diabetic patients' with proliferative retinopathies via a radial basis probabilistic neural network. In *International Conference on*

Intelligent Computing (pp. 115-126). Springer International Publishing.

23. Liu, C. L. (2010). A tutorial of the wavelet transform. NTUEE, Taiwan.

24. Osareh, A., Mirmehdi, M., Thomas, B., & Markham, R. (2002). Comparative exudate classification using support vector machines and neural networks. *Medical Image Computing and Computer-Assisted Intervention—MICCAI 2002*, **413-420**.

25. Mansour, R. F., Abdelrahim, E. M., & Al-Johani, A. S. (2013). Identification of diabetic retinal exudates in digital color images using support vector machine. *Journal of Intelligent Learning Systems and Applications*, **5**, **135-142**

26. Pass, G., & Zabih, R. (1999). Comparing images using joint histograms. *Multimedia systems*, **7(3)**, **234-240**.

27. Kälviäinen, R. V. J. P. H., & Uusitalo, H. (2007). DIARETDB1 diabetic retinopathy database and evaluation protocol. *Medical Image Understanding and Analysis* **2007**, **61**.

28. Dogra, R., & Gupta, N. (2014). Glowworm Swarm Optimization Technique for Optimal Power Flow, *Advance in Electronic and Electric Engineering*, **4 (2)**, **155-160**

29. Liu, J., Zhou, Y., Huang, K., Ouyang, Z., & Wang, Y. (2011). A glowworm swarm optimization algorithm based on definite updating search domains. *Journal of Computational Information Systems*, **7(10)**, **3698-3705**.

30. Zhou, Y., Luo, Q., & Liu, J. (2014). Glowworm swarm optimization for dispatching system of public transit vehicles. *Neural processing letters*, **40(1)**, **25-33**.